Proceedings of the 28th IEEE
EMBS Annual International Conference
New York City, USA, Aug 30-Sept 3, 2006

An Iterative Constrained Least Squares Filter for Ultrasound Image Deconvolution

Wee-Soon Yeoh*, Cishen Zhang†, and Ming Chen*
*School of Electrical and Electronic Engineering
†School of Electrical and Electronic Engineering & School of Chemical and Biomedical Engineering
Nanyang Technological University
Nanyang Avenue, Singapore 639798

***Abstract*— This paper describes how the recently developed constrained least squares (CLS) filtering algorithm can be made iterative to improve the resolution gain (RG) of medical ultrasound images. We propose the use of the iterative CLS (ICLS) filter, by incorporating the recently proposed ultrasound tissue model, to account for the random fluctuations of the tissue signal within the received ultrasound radio frequency (RF) echo signal. The resulting improvement in RG is demonstrated by eight different abdomen ultrasound images where progressive improvements in both the axial and lateral directions can be observed.**

I. Introduction

The ultrasound imaging is one of the most widely used medical modalities for diagnostic. Unfortunately, there are several limiting factors that can result in lower spatial resolution. These factors include the finite bandwidth of the scanner probe and the spreading of the ultrasonic pulse-echo wavelet through the tissue due to frequency-dependent attenuation, dispersive, and phase aberration [1], [2].

In the RF domain, the ultrasound image formation process can be modeled as a spatio-temporal convolution between the ultrasound pulse-echo wavelet, or point-spread function (PSF), and the tissue response [1]–[5]. Based on this, more recent works formulate the restoration of the tissue image as a deconvolution problem. An advantage of this approach is that, if the spatially variant two-dimensional (2-D) PSF is estimated accurately, high resolution of the deconvolved image can be achieved.

Recently, a CLS filter is proposed which incorporates a new ultrasound tissue model for the deconvolution [6]. The inclusion of this model into the received pulse-echo pressure field reveals that there are two different natures of noise sources existing in the received ultrasonic RF echo. One is inherent in the tissue response and the other is the measurement noise. And a desirable ultrasound image requires that effects of both kinds of noise be suppressed. The CLS filtering algorithm based on this new model combines the optimal Wiener filter to reduce the measurement noise and the constrained LS filter to suppress the fluctuations in the tissue signal.

In this paper, we propose an ICLS filtering algorithm that iteratively computes the CLS filtering algorithm on the error signal thereby improving the resultant deconvolution image resolution progressively in term of resolution gain (RG).

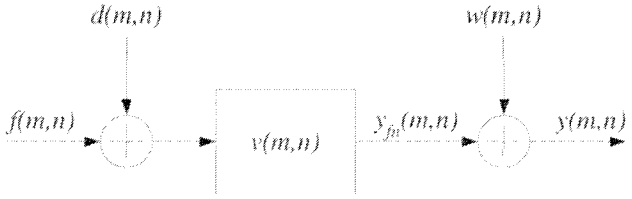

Fig. 1. Block diagram of the ultrasound convolution model.

The paper is organized as follows. Section II introduces the ultrasound tissue model, the convolution model of the RF echo, and a brief description of the CLS filtering algorithm. Section III presents the ICLS filtering algorithm. In Section IV, experiments and results of the proposed algorithm on real ultrasound RF data are presented. Finally, Section V concludes the paper.

II. Problem Formulation

Under the assumptions of linear propagation and weak scattering, an expression for the received pulse-echo pressure field in the RF domain was derived using the first-order Born approximation presented in a convolution model in the following form [1], [2], [4]–[6]:

$$y(m,n) = v(m,n) * s(m,n) + w(m,n), \qquad (1)$$

where m and n are discrete indices representing the sampled 2-D horizontal and vertical coordinates respectively, $y(m,n)$ is the ultrasound RF echo, $v(m,n)$ is the 2-D PSF, $s(m,n)$ is the tissue response, $w(m,n)$ is additive noise, and '$*$' denotes the discrete 2-D linear convolution.

Generally, the tissue signal is represented by scattered field as sum of the average field and the fluctuating field [7], or it is decomposed into a coherent field and a diffused component [8]. This means that $s(m,n)$ can be modeled as [6]:

$$s(m,n) = f(m,n) + d(m,n), \qquad (2)$$

where $f(m,n)$ is the noiseless tissue which is the signal to be displayed, and $d(m,n)$ is the diffused component is a random process [8]–[10]. Since the desired tissue image is $f(m,n)$ and it is a convolution component of $y(m,n)$, the process of recovering $f(m,n)$ from $y(m,n)$ is known as deconvolution. The block diagram of the ultrasound convolution model is shown in Fig. 1.

The proposed ICLS filtering algorithm of this paper for dealing with the blind deconvolution problem is an extension of the CLS filter described as follows. If the effects of noise are omitted, i.e.,$y_{fn}(m,n) = y(m,n)$, a good restoration should give a blurred estimate approximately given by:

$$v(m,n) * \breve{f}(m,n) = y_{fn}(m,n), \tag{3}$$

where $\breve{f}(m,n)$ denotes an estimate solution of $f(m,n)$. In the presence of the randomness in $y_{fn}(m,n)$, i.e., $v(m,n) * d(m,n)$, the application of an inverse filter can cause problems due to the exact fitting to the noisy data. A reasonable expectation for the restoration which accounts for the noise term is that it satisfies the following norm constrained condition:

$$||y_{fn}(m,n) - v(m,n) * \breve{f}(m,n)||^2 = ||v(m,n) * d(m,n)||^2, \tag{4}$$

where $||\cdot||$ is the L^2 norm. This implies that we select $\breve{f}(m,n)$ such that, if it is blurred by $v(m,n)$, the result will differ from $y_{fn}(m,n)$ as little as possible in the mean-square sense.

We proceed on to set up a constraint minimization problem by selecting a weighting function $\Omega(m,n)$ as a desired linear operation on $\breve{f}(m,n)$. The constrained least squares minimization problem minimizes the criteria function $||\Omega(m,n)||^2$ subject to the norm constraint (4) [11], [12].

Using the method of Lagrange multipliers gives the estimated noiseless tissue image:

$$\breve{f}(m,n) = \arg\min_{\breve{f}} \left\{ ||\Omega(m,n)||^2 + \lambda \left(\left|\left| y_{fn}(m,n) - v(m,n) * \breve{f}(m,n) \right|\right|^2 - ||v(m,n) * d(m,n)||^2 \right) \right\}, \tag{5}$$

where λ is the Lagrange multiplier.

Let F_2 denotes the 2-D Fourier transform, i.e., $Y(\omega_m,\omega_n) = \mathrm{F}_2[\,y(m,n)\,]$, $V(\omega_m,\omega_n) = \mathrm{F}_2[\,v(m,n)\,]$, $\mathrm{F}_2[\,\Omega(m,n)\,] = Q(\omega_m,\omega_n)\breve{F}(\omega_m,\omega_n)$, where '*' denotes complex conjugate, and $H(\omega_m,\omega_n)$ is the Wiener filter.

It has been shown in [6] that the Lagrangian minimization of (5) can lead to:

$$\breve{F}(\omega_m,\omega_n) = \frac{V(\omega_m,\omega_n)^* Y(\omega_m,\omega_n)}{|V(\omega_m,\omega_n)|^2 + \gamma \left| \frac{Q(\omega_m,\omega_n)}{V(\omega_m,\omega_n)\,H(\omega_m,\omega_n)} \right|^2}, \tag{6}$$

where $\gamma = 1/\lambda$ is the reciprocal Lagrange multiplier and must be adjusted iteratively to satisfy the constraint.

The derivation of the proposed ICLS filter is based on the CLS filter elaborated as follows. Let the estimated tissue image during the ith iteration be $\breve{F}_i(\omega_m,\omega_n) = F(\omega_m,\omega_n) - \Delta F_i(\omega_m,\omega_n)$. Applying the deconvolution algorithm derived in (6) iteratively, the error at the ith iteration being the difference between the observation and the re-blurred ith estimate and is given by:

$$\begin{aligned} \epsilon_i(\omega_m,\omega_n) &= Y(\omega_m,\omega_n) - V(\omega_m,\omega_n)\,\breve{F}_i(\omega_m,\omega_n) \\ &= V(\omega_m,\omega_n)\,[\Delta F_i(\omega_m,\omega_n) + D(\omega_m,\omega_n)] + W(\omega_m,\omega_n)\,. \end{aligned} \tag{7}$$

It is shown that (7) is of the same form as the model in Fig. 1. with $F(\omega_m,\omega_n)$ replaced by $\Delta F_i(\omega_m,\omega_n)$. Therefore, we may deduce an estimation of $\Delta F_i(\omega_m,\omega_n)$ following the form of (6) as below:

$$\Delta\breve{F}_i(\omega_m,\omega_n) = \frac{V(\omega_m,\omega_n)^*\,\epsilon_i(\omega_m,\omega_n)}{|V(\omega_m,\omega_n)|^2 + \gamma \left| \frac{Q(\omega_m,\omega_n)}{V(\omega_m,\omega_n)\,H(\omega_m,\omega_n)} \right|^2}. \tag{8}$$

Then, we can update our estimation of $F(\omega_m,\omega_n)$ as follows:

$$\breve{F}_{i+1}(\omega_m,\omega_n) = \breve{F}_i(\omega_m,\omega_n) + \Delta\breve{F}_i(\omega_m,\omega_n). \tag{9}$$

Because $\epsilon_{i+1}(\omega_m,\omega_n) = Y(\omega_m,\omega_n) - V(\omega_m,\omega_n) \times \breve{F}_{i+1}(\omega_m,\omega_n)$, by simple substitution of (9) into it, we obtain the following relation between the errors at ith and $(i+1)$th iterations:

$$\epsilon_{i+1}(\omega_m,\omega_n) = \frac{\gamma \left| \frac{Q(\omega_m,\omega_n)}{V(\omega_m,\omega_n)\,H(\omega_m,\omega_n)} \right|^2 \epsilon_i(\omega_m,\omega_n)}{|V(\omega_m,\omega_n)|^2 + \gamma \left| \frac{Q(\omega_m,\omega_n)}{V(\omega_m,\omega_n)\,H(\omega_m,\omega_n)} \right|^2}. \tag{10}$$

Since $|V(\omega_m,\omega_n)|^2 \geq 0$, $|Q(\omega_m,\omega_n)|^2 \geq 0$ and $\gamma|H(\omega_m,\omega_n)|^2 \geq 0$, it is shown that $|\epsilon_{i+1}(\omega_m,\omega_n)|^2 \leq |\epsilon_i(\omega_m,\omega_n)|^2$ and hence the error reduces with an increases in the number of iterations.

In practice, the true PSF, $V(\omega_m,\omega_n)$, is not known. Under this circumstance, its estimation $\breve{V}(\omega_m,\omega_n)$ is used in (6) and (8). This substitution imposes an unavoidable error to the estimation which can only be alleviated by the use of a better PSF estimation algorithm. In the following, we elaborate the accuracy of the iterative algorithm when it is equipped with the estimated PSF.

Let the estimated PSF deviate from the true PSF by $\Delta V(\omega_m,\omega_n)$ such that $\breve{V}(\omega_m,\omega_n) = V(\omega_m,\omega_n) - \Delta V(\omega_m,\omega_n)$. Thus, in the proposed iterative deconvolution algorithm, the error at the ith iteration is given by:

$$\begin{aligned} \epsilon_i(\omega_m,\omega_n) &= Y(\omega_m,\omega_n) - \breve{V}(\omega_m,\omega_n)\,\breve{F}_i(\omega_m,\omega_n) \\ &= \breve{V}(\omega_m,\omega_n)\,[\Delta F_i(\omega_m,\omega_n) + D(\omega_m,\omega_n)] \\ &\quad + \Delta V(\omega_m,\omega_n)\,[F(\omega_m,\omega_n) + D(\omega_m,\omega_n)] + W(\omega_m,\omega_n)\,. \end{aligned} \tag{11}$$

In this case, if we let $\zeta_i(\omega_m,\omega_n) = \epsilon_i(\omega_m,\omega_n) - \Delta V(\omega_m,\omega_n)\,[\,F(\omega_m,\omega_n) + D(\omega_m,\omega_n)\,]$, we will have:

$$\begin{aligned} \zeta_i(\omega_m,\omega_n) &= \breve{V}(\omega_m,\omega_n)\,[\,\Delta F_i(\omega_m,\omega_n) + D(\omega_m,\omega_n)\,] \\ &\quad + W(\omega_m,\omega_n)\,. \end{aligned} \tag{12}$$

Equation (12) is again of the same form as the proposed new model in Fig. 1 with $V(\omega_m,\omega_n)$ and $F(\omega_m,\omega_n)$ replaced by $\breve{V}(\omega_m,\omega_n)$ and $\Delta F_i(\omega_m,\omega_n)$ respectively. In this sense, we may deduce an estimation of $\Delta F_i(\omega_m,\omega_n)$ following the form of (8) with $\zeta_i(\omega_m,\omega_n)$ in place of $\epsilon_i(\omega_m,\omega_n)$. Thus, the estimated tissue signal is updated as

follows:

$$\begin{aligned}\breve{F}_{i+1}(\omega_m,\omega_n) &= \breve{F}_i(\omega_m,\omega_n) + \Delta\breve{F}_i(\omega_m,\omega_n) \\ &= \breve{F}_i(\omega_m,\omega_n) + \\ &\quad \frac{\breve{V}(\omega_m,\omega_n)^*\,\zeta_i(\omega_m,\omega_n)}{|\breve{V}(\omega_m,\omega_n)|^2+\gamma\left|\frac{Q(\omega_m,\omega_n)}{\breve{V}(\omega_m,\omega_n)\,H(\omega_m,\omega_n)}\right|^2} \\ &= \breve{F}_1(\omega_m,\omega_n) + \\ &\quad \frac{\breve{V}(\omega_m,\omega_n)^*\,\xi_i(\omega_m,\omega_n)}{|\breve{V}(\omega_m,\omega_n)|^2+\gamma\left|\frac{Q(\omega_m,\omega_n)}{\breve{V}(\omega_m,\omega_n)\,H(\omega_m,\omega_n)}\right|^2},\end{aligned} \tag{13}$$

where $\breve{F}_1(\omega_m,\omega_n) = \breve{F}(\omega_m,\omega_n)$ and $\xi_i(\omega_m,\omega_n)$ is given as follows:

$$\begin{aligned}\xi_i(\omega_m,\omega_n) = \sum_{j=1}^{i} \epsilon_j(\omega_m,\omega_n) - \\ i \times \Delta V(\omega_m,\omega_n)\,[\,F(\omega_m,\omega_n) + D(\omega_m,\omega_n)\,]\,.\end{aligned} \tag{14}$$

When there is no error in the 2-D PSF estimation, we will have $\Delta V(\omega_m,\omega_n)$=0. Thus, equation (14) reveals that an unavoidable error occurred in the iterative filtering algorithm due to an inaccuracy in the estimation of the 2-D PSF. This error appears in the right hand side of (14) associated with $\Delta V(\omega_m,\omega_n)$ and it increases along with the number of iterations.

III. EXPERIMENTAL RESULTS AND DISCUSSIONS

A set of eight different unfiltered RF data is recorded from the abdomen of adult volunteers with a VIVID3 (GE, Medical ultrasound, Inc.) commercial ultrasound scanner, equipped with a special data-transfer board. These data are obtained by a linear array probe, with a central frequency of about 3.5 MHz. The images are simple in visualizations and do not require a scan conversion stage. The data are acquired with a single transmission focal point, localized approximately at the center of the field of view. All the data are composed, on average, of 200 RF-line, each of 1024 sample points in length. The sampling rate and resolution are 20 MHz and 16-bit, respectively.

The convolution model assumes a spatially invariant 2-D PSF. However in the real ultrasound RF data, the 2-D PSF is expected to varying in some extent. Thus, we segment the whole piece of ultrasound RF data into various overlapping segments and each of these segments can be considered to be the convolved result of a spatially invariant 2-D PSF and the noisy tissue image. As the sample RF data is prolonged in the axial direction with a size of 1024 by 301, the segmentation is only performed in the axial direction.

In the experiment, the estimation of the 2-D PSF is accomplished using the complex cepstrum method [2], [5], [6]. Each 2-D PSF estimate is based on sampled RF data from a block of 32 x 64. This setting is obtained empirically and should be large enough to accommodate the spatial extent of the 2-D PSF throughout different imaging depth. The RF images are then segmented into various rectangular blocks of 70 % overlapping. Among them, thirty blocks that have envelope SNR closer to 1.91 are undergone the 2-D PSF estimation.

The Estimations are performed in the cepstral domain using a 2-D Butterworth lowpass filter that has an order of 5, and cutoff frequencies of 0.5 and 0.7 in the axial and lateral axes respectively. The active map in the weighted LS phase unwrapping algorithm [6], [13] is set to 100 % and 30 % in the axial and lateral axes respectively. The estimated PSFs are averaged to improve the robustness of the estimation. This method is proposed by Oppenheim and Schafer in [14] which shows that homomorphic estimation of the PSF is feasible in the cepstral domain. Under this circumstance, the 2-D PSF $V(\omega_m,\omega_n)$ is substituted by its estimation $\breve{V}(\omega_m,\omega_n)$.

The assessment of the ICLS filter performance is accomplished based on RG which is defined as the ratio of the correlation lengths of the RF data before and after deconvolution. It is computed for both the -5 dB and -10 dB correlation lengths of the RF data corresponding to the images before and after deconvolution. Defining the resolution at two different dB levels allows us to have a better idea of the shape of the 2-D autocovariance function (ACF). These computations are performed on both the axial slice, A_{00}, and lateral slice, L_{00}, where they are extracted through the peak of the 2-D ACF. Fig. 2 illustrates the computation of the RG based on the envelope of A_{00} and L_{00}.

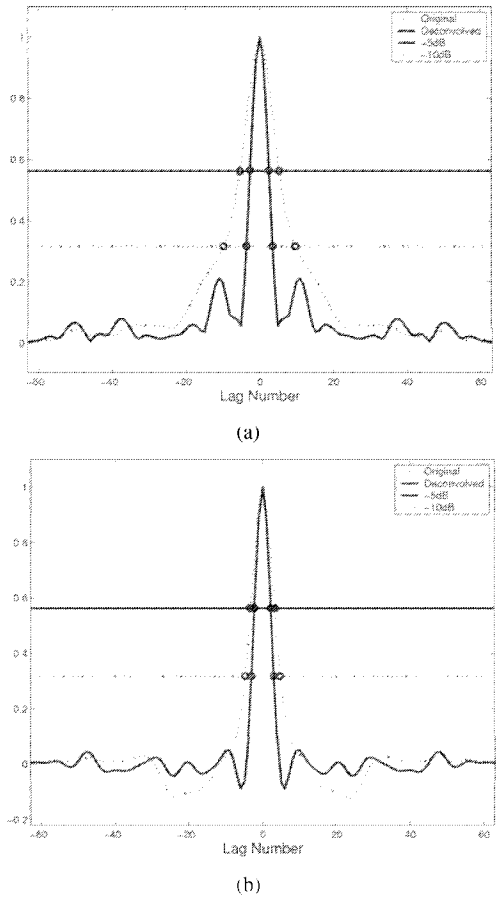

Fig. 2. Computation of the resolution gain based on the axial and lateral slices of the ACF. Envelopes of the (a) A_{00}, and (b) L_{00} corresponding to that of the original image (· · ·) and the deconvolved image ( ) with the RG_{-5dB} and RG_{-10dB} lines.

TABLE I

RESOLUTION GAINS OBTAINED DUE TO DECONVOLUTION USING THE PROPOSED CLS AND ICLS FILTERS COMPUTED IN THE RF DOMAIN. THESE VALUES ARE TABULATED IN TERMS OF MEAN ± ONE STANDARD DEVIATION.

Description	Axial slice, A_{00}		Lateral slice, L_{00}	
	RG_{5dB}	RG_{10dB}	RG_{5dB}	RG_{10dB}
CLS filter	1.7214 ± 0.2266	1.9341 ± 0.5954	1.3151 ± 0.1654	1.3671 ± 0.2036
ICLS filter, 10 iterations	1.8330 ± 0.2372	2.1635 ± 0.4732	1.4461 ± 0.2555	1.5091 ± 0.3069
ICLS filter, 20 iterations	1.8565 ± 0.2548	2.1923 ± 0.4925	1.4784 ± 0.2857	1.5465 ± 0.3421
ICLS filter, 30 iterations	1.8679 ± 0.2651	2.2047 ± 0.5040	1.4999 ± 0.3068	1.5710 ± 0.3675

Table I tabulates RG under different iterations. As shown, the results clearly indicate a progressively improvement in RG. The original and the deconvolved images under 30 iterations is depicted in Fig. 3(a) and Fig. 3(b) respectively. The figure can show that the size of the speckle is reduced and the tissue structures are better defined in the deconvolved ultrasound image.

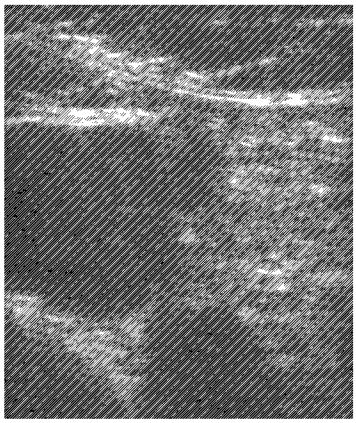

(a)

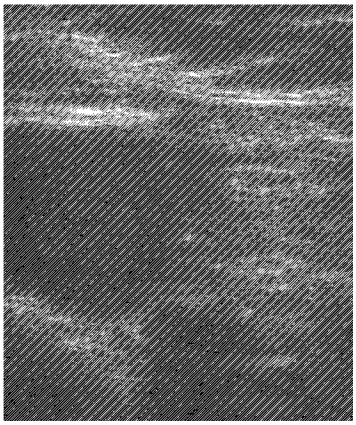

(b)

Fig. 3. Ultrasound image of the human abdomen acquired by the linear array transducer. (a) Original, and (b) ICLS filtered image, $\gamma=10^{2}$, and 30 iterations.

IV. CONCLUSION

This paper has presented an ICLS filtering algorithm which can show progressively improvement of the deconvolved ultrasound image quality in terms of resolution gain. It is an extension of the CLS filter which combines optimal Wiener filter and constrained LS filtering algorithms for the estimation of the tissue image. Our experimental results have achieved an improvement in the deconvolved image quality.

In this paper, we have not addressed the error issue that will incur using the estimated 2-D PSF. Since the true 2-D PSF in the tissue cannot be known, this issue will be addressed in future through analytical and simulated studies.

REFERENCES

[1] U. R. Abeyratne, A. P. Petropulu, and J. M. Reid, "Higher order spectra based deconvolution of ultrasound images," *IEEE Trans. Ultrason., Ferroelect., Freq. Contr.*, vol. 42, no. 6, pp. 1064–1075, Nov. 1995.

[2] T. Taxt and G. V. Frolova, "Noise robust one-dimensional blind deconvolution of medical ultrasound images," *IEEE Trans. Ultrason., Ferroelect., Freq. Contr.*, vol. 46, no. 2, pp. 291–299, 1999.

[3] J. A. Jensen, "A model for the propagation and scattering of ultrasound in tissue," *J. Acoust. Soc. Amer.*, vol. 89, no. 1, pp. 182–190, Jan. 1991.

[4] ——, "Deconvolution of ultrasound images," *Ultrasound Imaging*, vol. 14, pp. 1–5, 1992.

[5] T. Taxt, "Restoration of medical ultrasound images using two-dimensional homomorphic deconvolution," *IEEE Trans. Ultrason., Ferroelect., Freq. Contr.*, vol. 42, no. 4, pp. 543–554, 1995.

[6] W. S. Yeoh and C. Zhang, "Constrained least squares filtering for ultrasound image deconvolution," in *Proc. IEEE 27th International Conf. of IEEE-EMBS*, Shanghai, China, Dec. 2005.

[7] M. F. Insana, D. G. B. R. F. Wagner, and T. J. Hall, "Describing small-scale structure in random media using pulse-echo ultrasound," *J. Acoust. Soc. Amer.*, vol. 87, no. 1, pp. 179–192, Jan. 1990.

[8] G. Georgiou and F. S. Cohen, "Statistical characterization of diffuse scattering in ultrasound images," *IEEE Trans. Ultrason., Ferroelect., Freq. Contr.*, vol. 45, no. 1, pp. 57–64, Jan. 1998.

[9] U. R. Abeyratne, A. P. Petropulu, and J. M. Reid, "On modeling the tissue response from ultrasonic b-scan images," *IEEE Trans. Med. Imag.*, vol. 15, no. 4, pp. 479–490, Aug. 1996.

[10] P. M. Shankar, "A general statistical model for ultrasonic backscattering from tissues," *IEEE Trans. Ultrason., Ferroelect., Freq. Contr.*, vol. 47, no. 3, pp. 727 736, May 2000.

[11] R. C. Gonzalez and R. E. Woods, *Digital image processing*. Upper Saddle River: NJ: Prentice-Hall, 2002.

[12] J. Biemond, R. L. Lagendijk, and R. M. Mersereau, "Iterative methods for image deblurring," in *Proc. IEEE*, vol. 78, no. 5, May 1990, pp. 856–883.

[13] D. C. Ghiglia and M. D. Pritt, *Two-dimensional phase unwrapping: Theory, algorithms and software*. John Wiley & Sons, 1998.

[14] A. V. Oppenheim and R. W. Schafer, *Discrete-time signal processing*. Englewood Cliffs: NJ: Prentice-Hall, 1989.